BELLE2-NOTE-PL-2020-002
Version 1.1
April 6, 2020

Plots for approval: Full Event Interpretation Reconstruction Performance with 8.7 fb^{-1} of Phase III data in bucket 8 and proc 10.

Belle II collaboration

Abstract

This note presents hadronic FEI performance plots associated with the analysis work presented in BELLE2-NOTE-PH-2019-031 for approval made using proc 10 and bucket 8 data (8.7 fb^{-1}) of early phase III data. Plots include a comparison of the classifier output for the tag-side B mesons in data to the shape expected from simulation, fits to the beam constrained mass distributions in data in different purity regions, the beam constrained mass distributions of neutral and charged tag-side B mesons in data with different categories of tag-side B meson decay modes stacked and, finally, fits are shown to the lepton momentum in the signal B rest frame for a reconstructed signal side $B \to X\ell\nu$.

1. PLOTS FOR APPROVAL

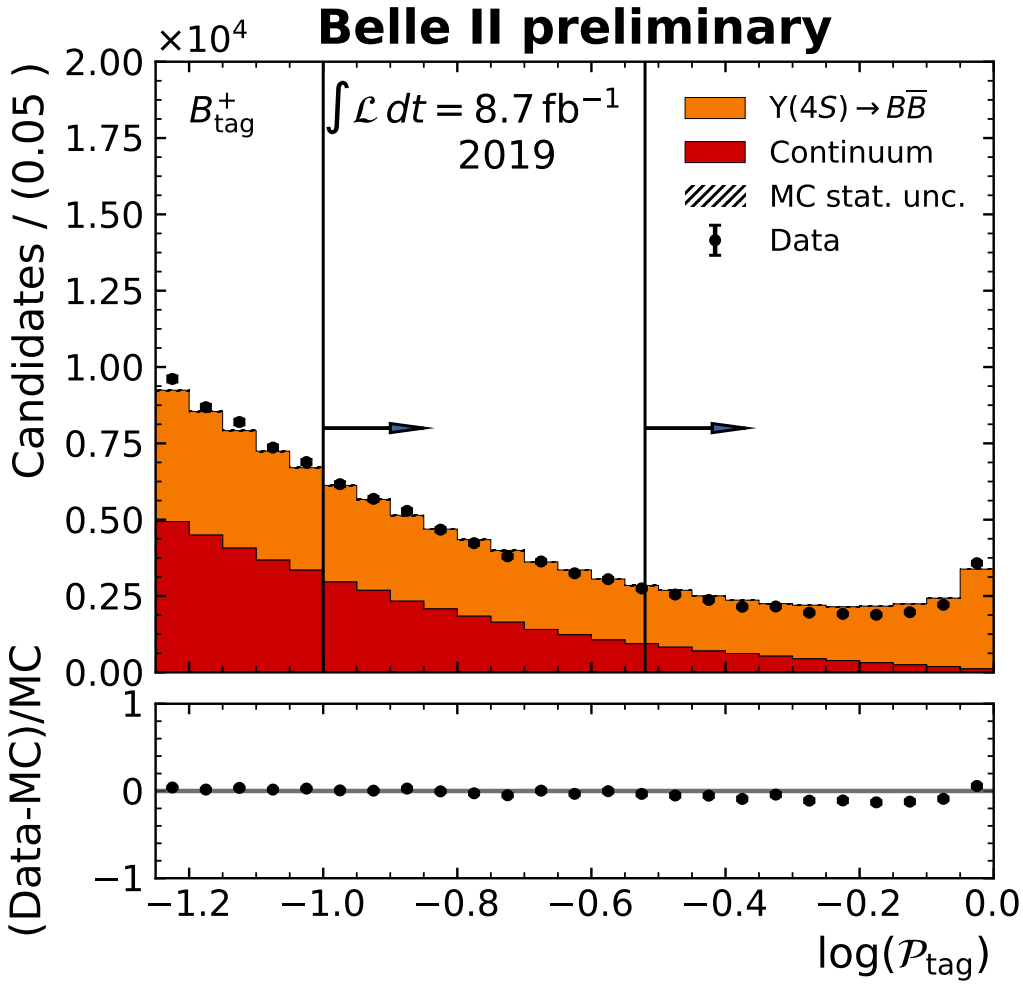

FIG. 1: Comparison of the distribution of $\log \mathcal{P}$ in early phase III data to the shape expectation from simulation. Here $\log \mathcal{P}$ is the logarithm of the tag-side B^+ meson classifier output, $\mathcal{P}$. Simulated Monte Carlo data here is scaled to the normalisation of the data making this purely a shape comparison. Two cuts choices are illustrated, which correspond to cuts of $\mathcal{P} > 0.1$ and $\mathcal{P} > 0.3$. Selections on $\mathcal{P}$ can be used to remove background from incorrectly reconstructed tag-side B mesons. Additional selections include an asymmetric selection on the beam energy difference to lie in the region $-0.15 < \Delta E < 0.1$ GeV and a loose selection on an event level normalised Fox Wolfram moment, $R2 < 0.3$, to suppress continuum. In addition, a best candidate candidate selection is made selecting the reconstructed B meson tag-side candidate in each event with the highest $\mathcal{P}$.

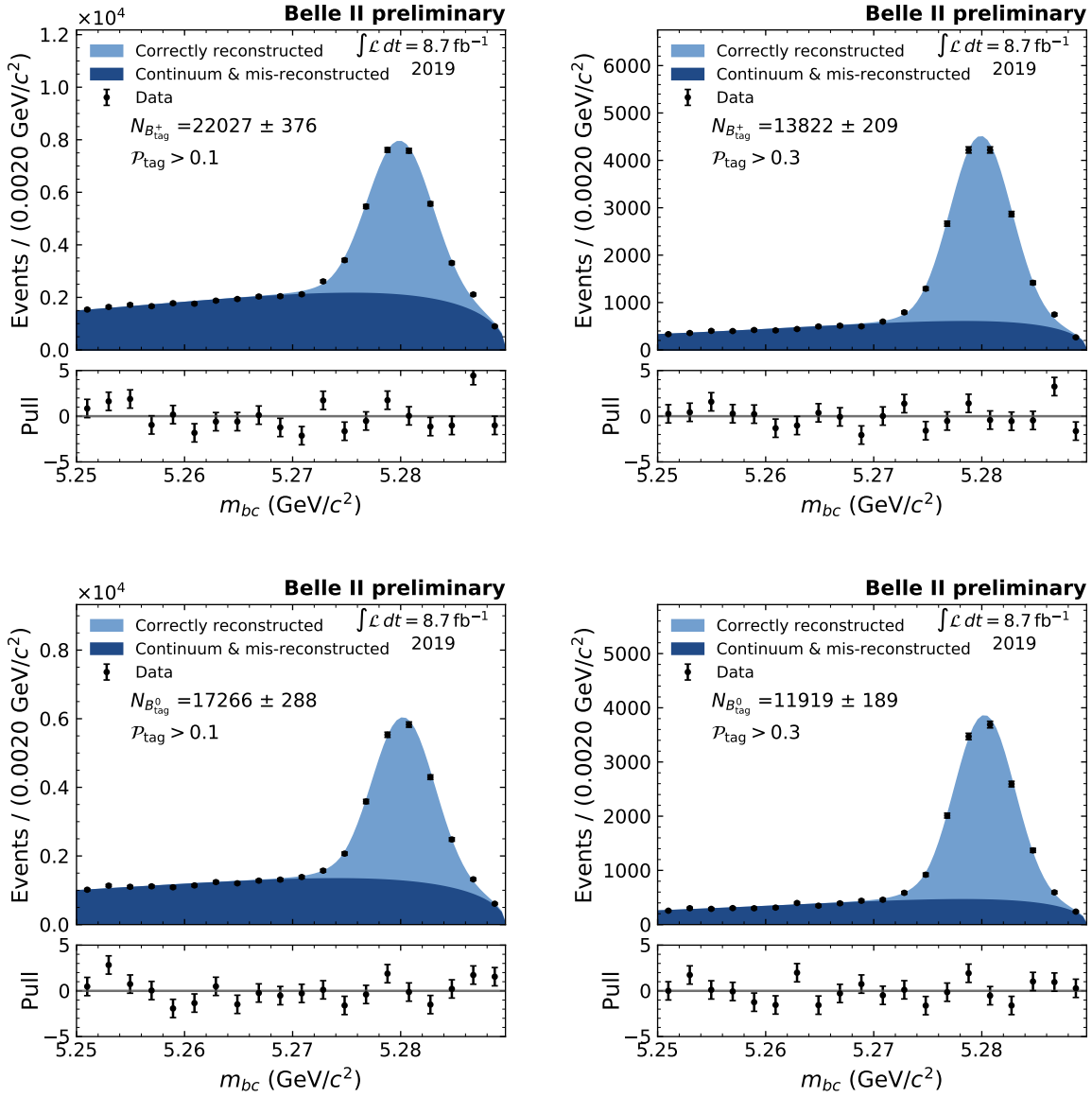

FIG. 2: Fits to the beam constrained mass, m_{bc}, distribution of reconstructed B^+ (top) and B^0 (bottom) tag-side B mesons in data. Here correctly reconstructed signal is modelled with a Crystal Ball and mis-reconstructed B mesons and continuum are modelled with an Argus shape. While the mean and sigma paramters of the Crystal Ball are free to float, the tail parameters are fixed based on fits to correctly reconstructed tag-side candidates in simulation. Two choices of selection are employed on the B meson classifier output, $\mathcal{P}$, a looser selection of $\mathcal{P} > 0.1$ (left) and a tighter selection of $\mathcal{P} > 0.3$ (right). The corresponding yields of correctly reconstructed B^+ or B^0 mesons are displayed on each plot. Additional selections include an asymmetric selection on the beam energy difference to lie in the region $-0.15 < \Delta E < 0.1$ GeV and a loose selection on an event level normalised Fox Wolfram moment, $R2 < 0.3$, to suppress continuum. In addition, a best candidate candidate selection is made selecting the reconstructed B meson tag-side candidate in each event with the highest $\mathcal{P}$.

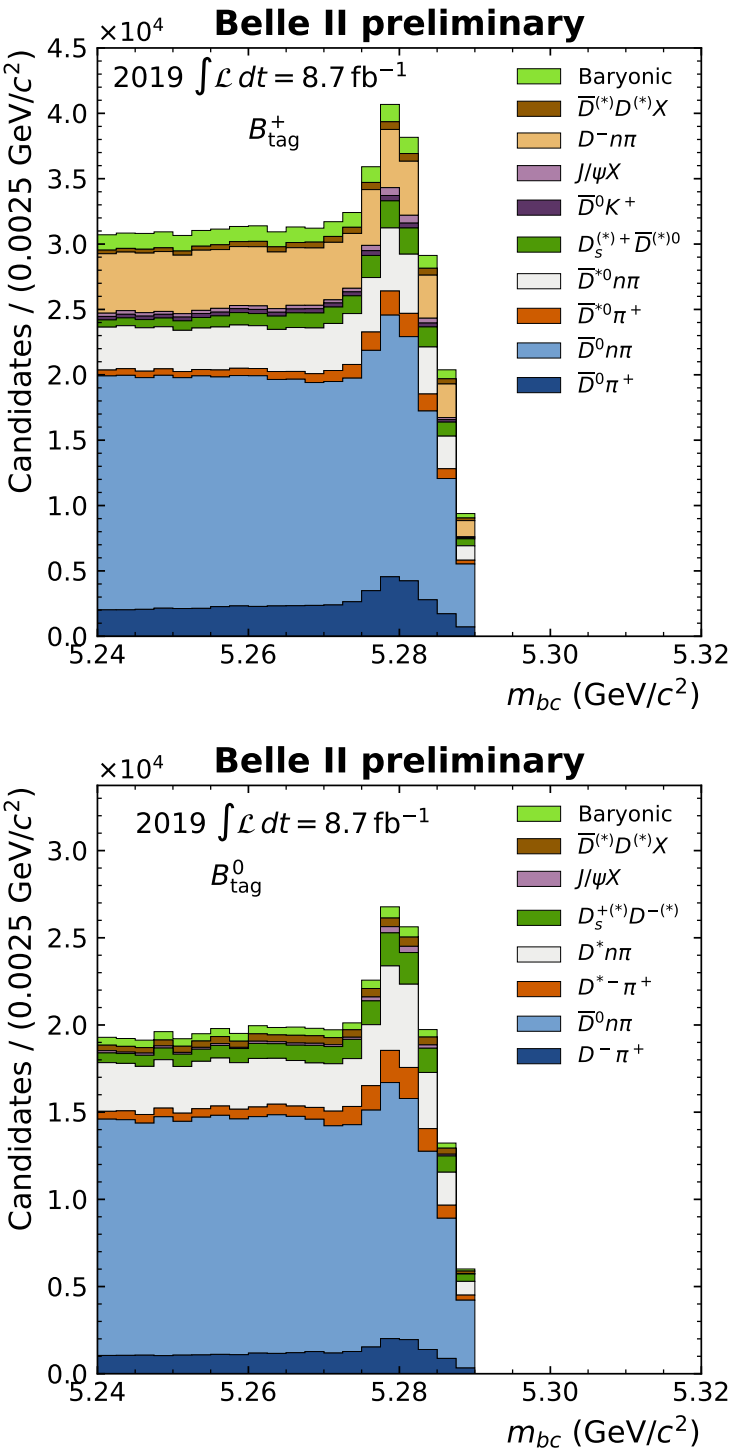

FIG. 3: The m_{bc} distribution of tag-side B^+ (top) and B^0 (bottom) mesons is shown in data with a selection of the tag-side B meson classifer $\mathcal{P}$ to be greater than 0.1. The Full Event Interpretation reconstructs 29 and 26 hadronic B^+ and B^0 modes, respectively. Contributions from 10 (8) different categories of charged (neutral) modes are stacked including the recently added modes contraining baryons. Additional selections include an asymmetric selection on the beam energy difference to lie in the region $-0.15 < \Delta E < 0.1$ GeV and a loose selection on an event level normalised Fox Wolfram moment, $R2 < 0.3$, to suppress continuum. In addition, a best candidate candidate selection is made selecting the reconstructed B meson tag-side candidate in each event with the highest $\mathcal{P}$.

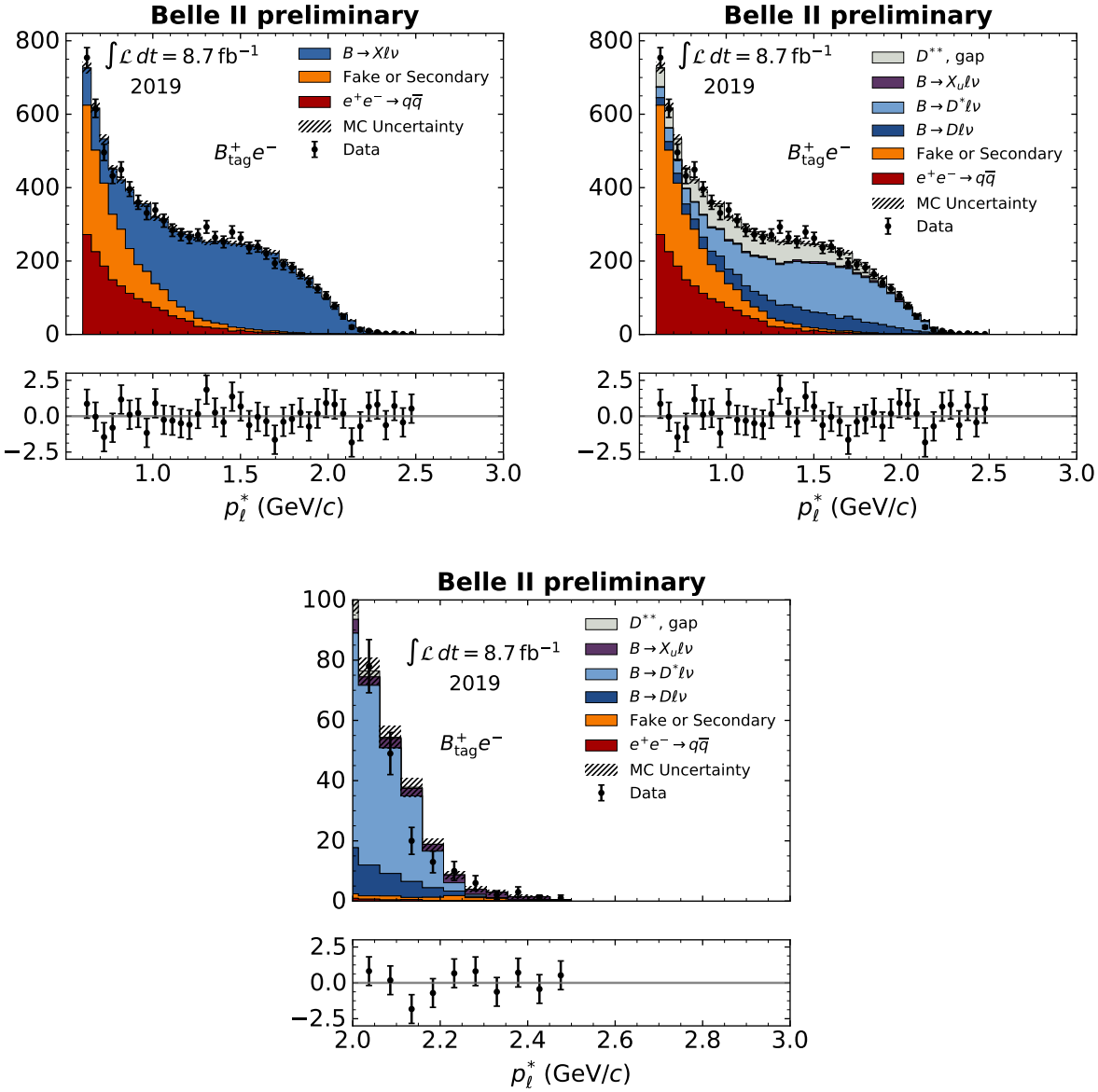

FIG. 4: Fit to the lepton momentum, p^*_ℓ, in the B rest frame for $B^+_{\mathrm{tag}}e^-$ combinations. Here a signal-side electron has been selected after reconstructing a tag-side B meson hadronically with the Full Event Interpretation. Selections on the electon include $p^*_e > 0.6$ GeV/c and electronID > 0.9. Selections on the tag-side B meson include an asymmetric selection on the beam energy difference to lie in the region $-0.15 < \Delta E < 0.1$ GeV, a selection of $m_{bc} > 5.27$ GeV/c^2 and a loose selection on an event level normalised Fox Wolfram moment, $R2 < 0.3$, to suppress continuum. Finally best candidate selections are made on both the tag-side B meson classifier $\mathcal{P}$ and p^*_e, which select the highest value candidates in these variables. The $B \to X\ell\nu$ signal template is broken into four components ($D\ell\nu$, $D^*\ell\nu$, $X_u\ell\nu$ and $D^{**}\ell\nu$ + gap) in the fit as seen in the top left plot, which are governed by three fractions. Zooming in to the endpoint region the contribution of $X_u\ell\nu$ becomes visible due to its higher kinematic endpoint than $X_c\ell\nu$. The binned fitting procedure includes the impact of several systematic sources of uncertainties on histogram templates by including nuissance parameters for each bin of a fit template. Systematic uncertainties considered include MC statistical uncertainties, PID efficiency and fake rate uncertainties and finally the form factors of $B \to D^{(*)}\ell\nu$ decays.

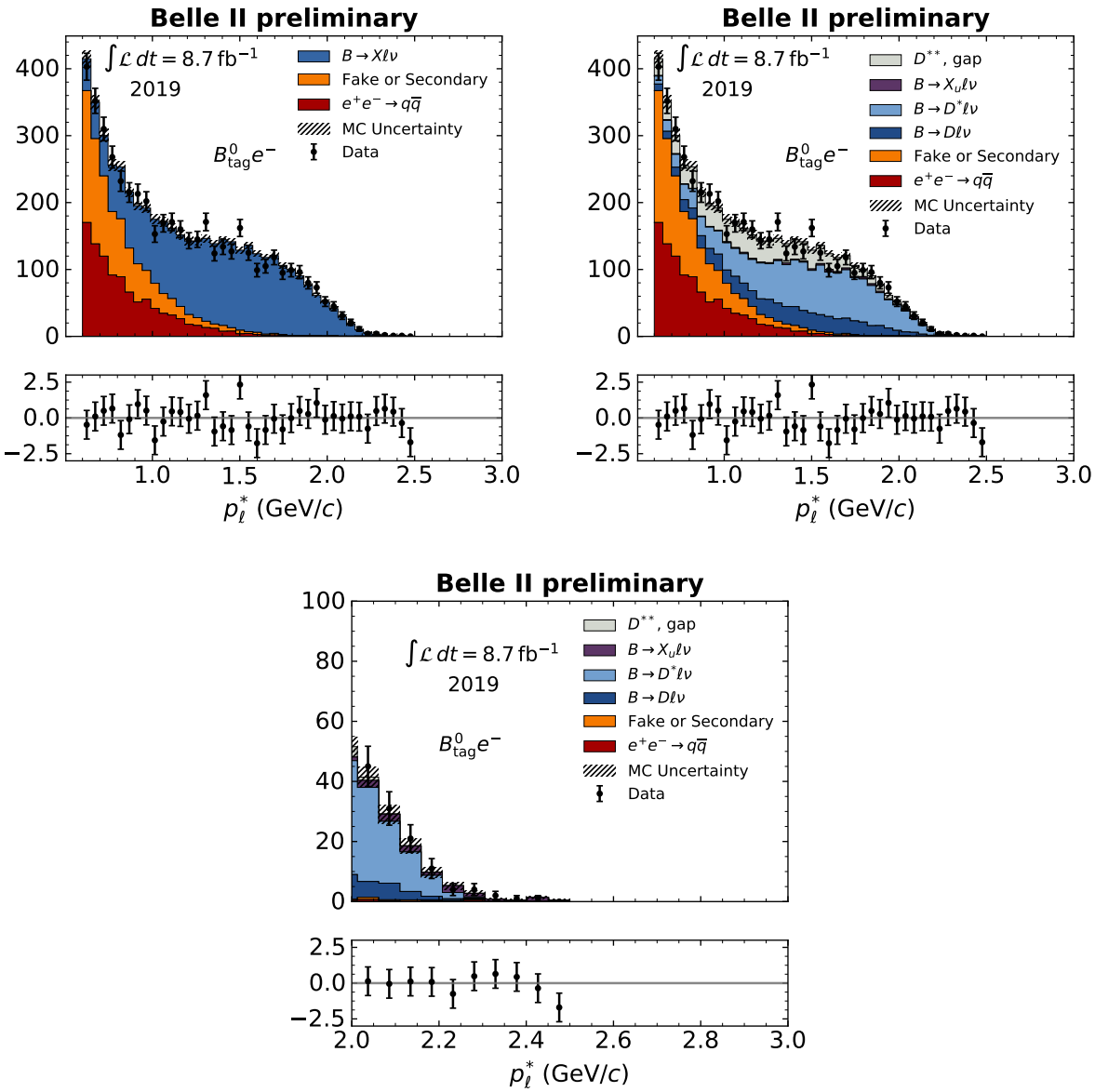

FIG. 5: Fit to the lepton momentum, p^*_ℓ, in the B rest frame for $B^0_{\mathrm{tag}}e^-$ combinations. Here a signal-side electron has been selected after reconstructing a tag-side B meson hadronically with the Full Event Interpretation. Selections on the electon include $p^*_e > 0.6$ GeV/c and electronID > 0.9. Selections on the tag-side B meson include an asymmetric selection on the beam energy difference to lie in the region $-0.15 < \Delta E < 0.1$ GeV, a selection of $m_{bc} > 5.27$ GeV/c^2 and a loose selection on an event level normalised Fox Wolfram moment, $R2 < 0.3$, to suppress continuum. Finally best candidate selections are made on both the tag-side B meson classifier $\mathcal{P}$ and p^*_e, which select the highest value candidates in these variables. The $B \to X\ell\nu$ signal template is broken into four components ($D\ell\nu$, $D^*\ell\nu$, $X_u\ell\nu$ and $D^{**}\ell\nu$ + gap) in the fit as seen in the top left plot, which are governed by three fractions. Zooming in to the endpoint region the contribution of $X_u\ell\nu$ becomes visible due to its higher kinematic endpoint than $X_c\ell\nu$. The binned fitting procedure includes the impact of several systematic sources of uncertainties on histogram templates by including nuissance parameters for each bin of a fit template. Systematic uncertainties considered include MC statistical uncertainties, PID efficiency and fake rate uncertainties and finally the form factors of $B \to D^{(*)}\ell\nu$ decays.

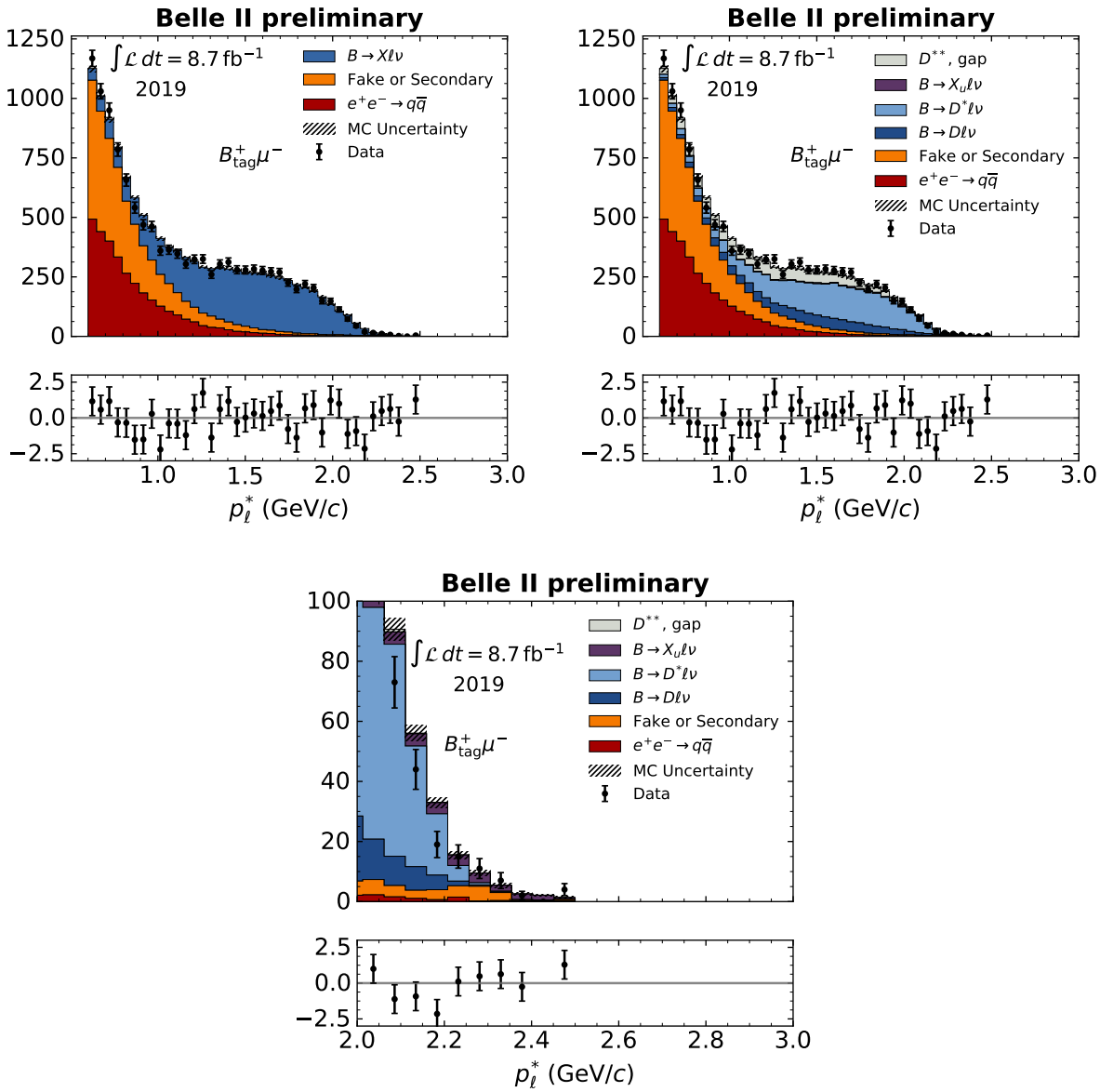

FIG. 6: Fit to the lepton momentum, p^*_ℓ, in the B rest frame for $B^+_{\mathrm{tag}}\mu^-$ combinations. Here a signal-side muon has been selected after reconstructing a tag-side B meson hadronically with the Full Event Interpretation. Selections on the electon include $p^*_\mu > 0.6$ GeV/c and muonID > 0.9. Selections on the tag-side B meson include an asymmetric selection on the beam energy difference to lie in the region $-0.15 < \Delta E < 0.1$ GeV, a selection of $m_{bc} > 5.27$ GeV/c^2 and a loose selection on an event level normalised Fox Wolfram moment, $R2 < 0.3$, to suppress continuum. Finally best candidate selections are made on both the tag-side B meson classifier $\mathcal{P}$ and p^*_μ, which select the highest value candidates in these variables. The $B \to X\ell\nu$ signal template is broken into four components ($D\ell\nu$, $D^*\ell\nu$, $X_u\ell\nu$ and $D^{**}\ell\nu$ + gap) in the fit as seen in the top left plot, which are governed by three fractions. Zooming in to the endpoint region the contribution of $X_u\ell\nu$ becomes visible due to its higher kinematic endpoint than $X_c\ell\nu$. The binned fitting procedure includes the impact of several systematic sources of uncertainties on histogram templates by including nuissance parameters for each bin of a fit template. Systematic uncertainties considered include MC statistical uncertainties, PID efficiency and fake rate uncertainties and finally the form factors of $B \to D^{(*)}\ell\nu$ decays.

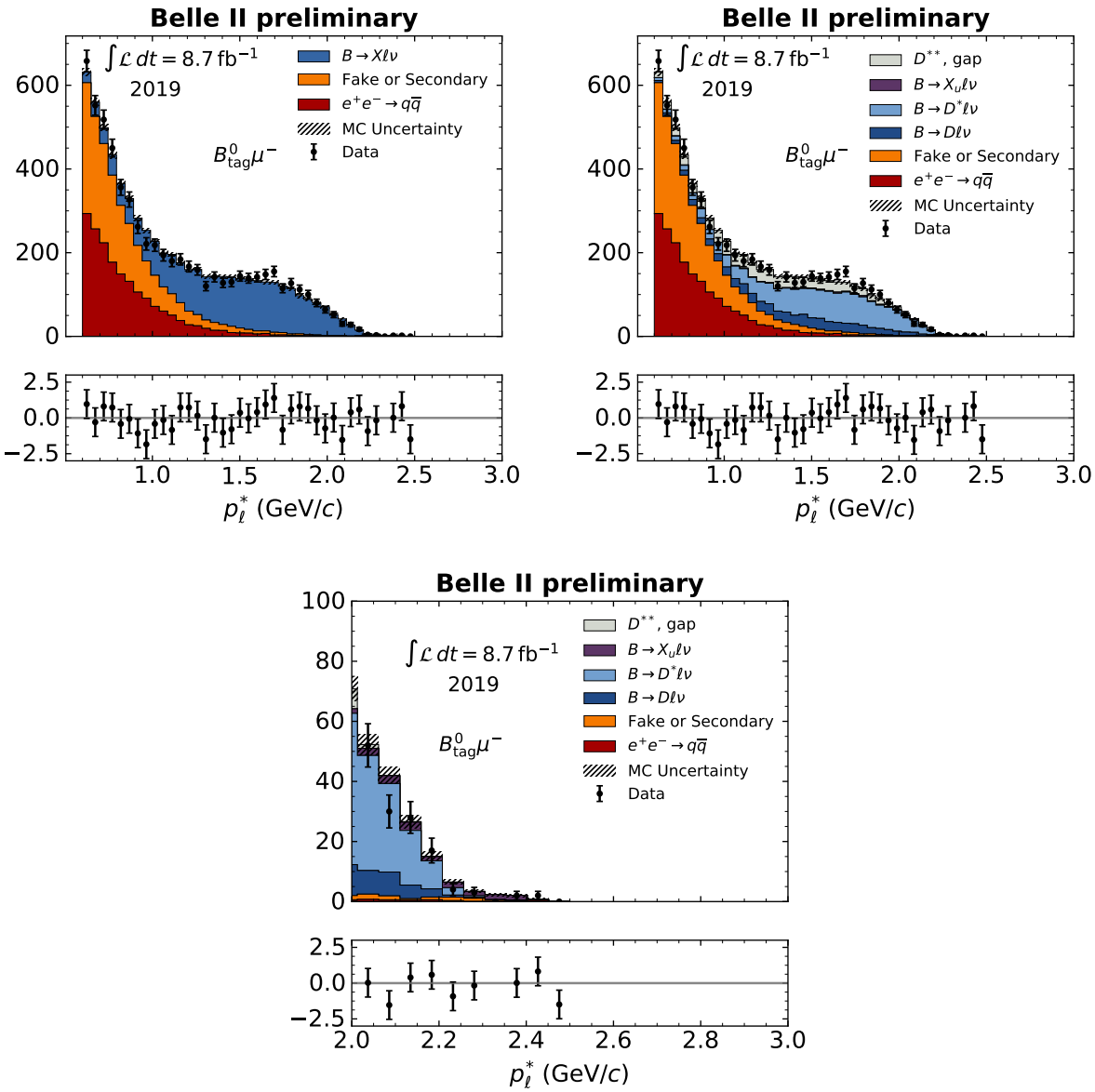

FIG. 7: Fit to the lepton momentum, p^*_ℓ, in the B rest frame for $B^0_{\mathrm{tag}}\mu^-$ combinations. Here a signal-side muon has been selected after reconstructing a tag-side B meson hadronically with the Full Event Interpretation. Selections on the electon include $p^*_\mu > 0.6$ GeV/c and muonID > 0.9. Selections on the tag-side B meson include an asymmetric selection on the beam energy difference to lie in the region $-0.15 < \Delta E < 0.1$ GeV, a selection of $m_{bc} > 5.27$ GeV/c^2 and a loose selection on an event level normalised Fox Wolfram moment, $R2 < 0.3$, to suppress continuum. Finally best candidate selections are made on both the tag-side B meson classifier $\mathcal{P}$ and p^*_μ, which select the highest value candidates in these variables. The $B \to X\ell\nu$ signal template is broken into four components ($D\ell\nu$, $D^*\ell\nu$, $X_u\ell\nu$ and $D^{**}\ell\nu$ + gap) in the fit as seen in the top left plot, which are governed by three fractions. Zooming in to the endpoint region the contribution of $X_u\ell\nu$ becomes visible due to its higher kinematic endpoint than $X_c\ell\nu$. The binned fitting procedure includes the impact of several systematic sources of uncertainties on histogram templates by including nuissance parameters for each bin of a fit template. Systematic uncertainties considered include MC statistical uncertainties, PID efficiency and fake rate uncertainties and finally the form factors of $B \to D^{(*)}\ell\nu$ decays.